

Simulation Of An Efficient AC–DC Step-Up Converter For Low-Voltage Energy Harvesting

G. Laxminarayana¹, G.Bhargavi²

Assistant Professor, Dept.of EEE, Aurora's Engineering College, Bhongir, India¹

M.Tech Scholar, Dept.of EEE, Aurora's Engineering College, Bhongir, India²

Abstract

In this paper direct AC to DC is converted by proposed model from low AC voltage to high DC voltage in single stage conversion. And this paper presents an efficient AC to DC power that avoids the bridge rectification and directly converts low AC input voltage to high DC output voltage. This proposed converter consists boost converter and buck-boost converter both are connected in parallel to process the positive and negative half cycles of the input voltage. Analysis of the converter is carried out. Simulation results are presented to validate the proposed converter topology and control scheme.

Index Terms—AC–DC conversion, boost converter, energy harvesting, low power, low voltage, power converter control.

I. INTRODUCTION

Normally self powered devices harvest the ambient energies by microgenerators and having without any continuous power supply. Many types of microgenerators used for harvesting different forms of ambient energies [1]-[8]. The types of generators are electromagnetic, electrostatic and piezoelectric [5]-[10],[12]-[16]. Compare with all types of microgenerators electromagnetic microgenerators have the highest energy density. In this study electromagnetic generator is considered. The power level of inertial microgenerators is very low ranging from few micro watts to tens of milliwatts. In practical, electromagnetic micro generators are spring-mass-damper based resonance system shown in fig(1). In this, the small amplitude mechanical vibrations are amplified into larger amplitude translation movements. The functionality of the power converter is important than the maximum energy conversion. The output voltage of electromagnetic microgenerator is ac type but all electronic loads require dc voltage for further operation. Due to the practical size limitations the outputs of electromagnetic micro generator is very low(few 100mv), where the electronic loads require higher dc voltage(3.3v)

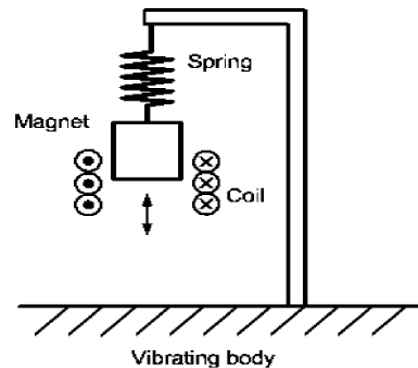


Fig 1. Schematic diagram of a resonance inertial microgenerator

In conventional power converters the ac –to–dc conversion is taken place by two stages that are first, diode bridge rectification and second power converters (standard buck or boost converter) to boost the output voltage(fig.2.). the existing power converter model have the major disadvantages that are first, the diode bridge rectification is not feasible for very low voltage electromagnetic microgenerators. Second, if diode bridge rectification is feasible, the forward voltage drops in the diode will cause a large amount of losses and make the power converter is inefficient.

To achieve the problems of the previous converter model direct ac-to-dc is proposed [10],[13],[15]. In this proposed converter model, bridge rectification is avoided and the microgenerator power is processed by single stage boost type power converter (fig3). In this type power converter the output dc split into two series connected capacitors and each capacitor charged for only one half cycle the microgenerator output voltage. The time periods of the resonance-based microgenerators output voltages are normally milliseconds, very large voltage drops will occur in the capacitors during the half cycles when the capacitors are not charged by the converter. In practical, large capacitors will required to achieve the allowable voltage ripple at dc bus output. This is not applicable for microgenerators because of practical size limitations.

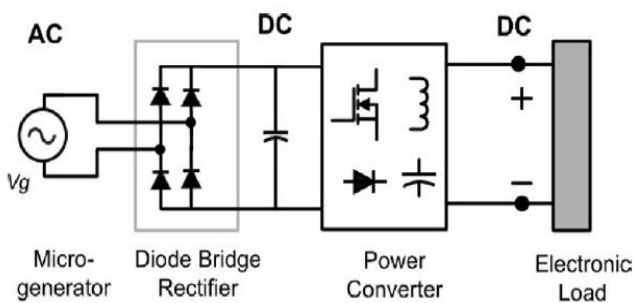


Fig 2. Conventional two stage power conversion model

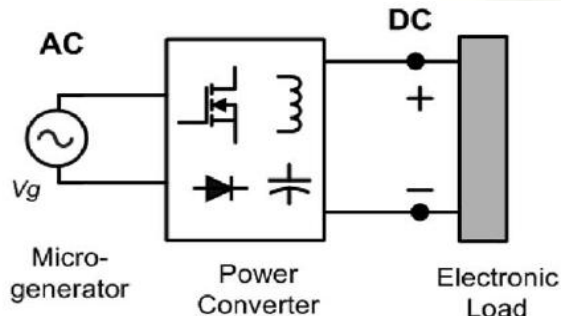


Fig 3. Proposed converter model (Direct ac-to-dc conversion)

The direct ac-to-dc converter is proposed in [21]. The proposed converter represented in fig4. The circuit consists of boost converter (Switch S_1 , inductor L_1 , Diode D_1) and buck- boost converter (Switch S_2 , inductor L_2 , Diode D_2). These two converters are connected in parallel. The operation of the converter model consists total four modes. For positive half cycle boost converter switch S_1 is turned ON, and inductor L_1 stores the energy and discharges through the Diode D_1 and Capacitor. For negative half cycle buck-boost converter Switch S_2 is turned ON, and inductor L_2 stores the energy and discharges through Diode D_2 and capacitor.

The converter is designed to operate in DCM mode. By this mode of operation switching losses and diode reverse recovery will be reduced. And the control scheme of the DCM is simpler than the CCM. For constant duty cycle operation DCM operation , the input current of the converter is proportional to the input voltage at every switching cycle.

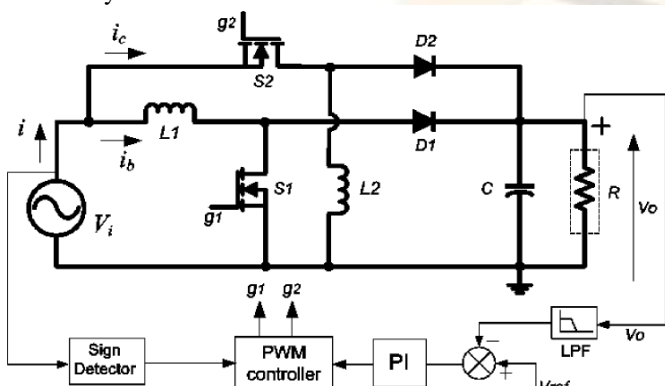


Fig 4. Proposed direct ac-to-de model.

II. DIRECT AC-TO-DC CONVERTER

The proposed power converter is direct ac-to-dc power consisting of one boost converter and one buck-boost converter. These two converters are connected in parallel. The operation of the circuit is discussed in[21].

A. Converter analysis

Consider the input current waveform of the converter as shown in Fig. 5(a). It can be noted that during the boost converter operation, the input current i and the boost inductor current ($iL1$) are equal, but during the buck-boost converter operation, the input current i and the current in buck-boost inductor ($iL2$) are not equal. This is because, in the buck-boost converter the input current becomes zero during the switch turn OFF period (T_{OFF}). Therefore, in a switching cycle, the energy transferred to the output by a buck-boost converter is equal to the energy stored in the inductor, whereas, in the boost converter, the energy transferred to the output is more than the energy stored in the inductor. Hence, for the equal duty cycles, input voltages and inductor values ($L1 = L2$), the total powers delivered by the two converters over an input voltage cycle are not equal. In this section, analyses of the converters are carried out and the relations between the control and circuit parameters of the boost and the buck-boost converters pertaining to the input power and the output power are obtained.

B. Converter analysis and control

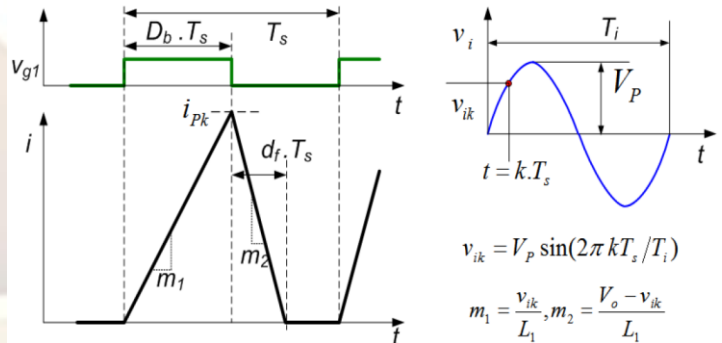


Fig. 5: Input current, gate drive signal and input voltage during a boost converter switching cycle.

Consider the input current waveform of the converter and various variables as defined in Fig 4. The average input power, P_{ib} , of the converter can be obtained as :

$$P_{ib} = \frac{V_p^2 \cdot D_b^2 T_s}{4L_1} \beta \quad (1)$$

$$\beta = (1/\pi) \int_0^{2\pi} \sin^2 \theta \cdot [1 - (V_p/V_0) \cdot \sin \theta]^{-1} dt$$

where, $\Theta = 2\pi.t/T_i$. It can be noted that in the above equation, (1), β is constant for fixed V_p and V_o . In steady state, the ratio of the duty cycle of the boost converter (D_b) and the duty ratio for the buck-boost converter, D_c , can be obtained (2).

$$\frac{D_c}{D_b} = \sqrt{\frac{L_2}{L_1}} \cdot \beta \quad (2)$$

From the above equation (2), two different schemes can be proposed to control the converter. In Scheme 1, the values of the inductors are set to be equal ($L_2 = L_1$). But the converters are controlled with different duty cycles, which satisfy the condition: $D_c = D_b \sqrt{\beta}$. In Scheme 2, both the boost and the buck-boost converter are controlled with same duty cycle ($D_b = D_c$). To achieve this, the inductor values are chosen to satisfy the condition: $L_1 = \beta L_2$. It can be seen from (1) that with higher value voltage step-up ratio the duty ratios of the two converters become almost equal. This is assistive for the target application where the very low voltage is stepped up to a much higher dc output voltage.

III. SIMULATION RESULTS

A resonance-based electromagnetic microgenerator, producing 400 mV peak sinusoidal output voltage, with 100Hz frequency is considered in this study for verification of the proposed converter topology (see Fig. 4). The closed-loop simulation of the converter is carried out based on the control schemes presented in. The reference output voltage (V_{ref}) is considered to be 3.3 V. The energy-harvesting converter is designed for supplying power to a 200Ω load resistance, hence, supplying about 55 mW of output power.

The simulation model of the proposed energy harvesting conveter and its control scheme shown in fig.6. The sensed output voltage of the converter is processed by a low-pass filter. The processed signal is compared with the reference voltage V_{ref} . The error signal is used by the PI controller to estimate the control voltage that is compared with a saw-tooth waveform in the pulse width modulator (PWM). The pulse signal produced by the PWM is fed to the two buffers that can be enabled by external signals. The comparators in the polarity detector unit enable the appropriate buffers to produce the gate pulses ($V_g 1$ and $V_g 2$) that control the MOSFETs of the boost and buck-boost converter during appropriate half cycles. In this

study, the resonance-based electromagnetic microgenerator is modeled as an ac voltage source. A signal generator followed by a high-current buffer is used to realize the microgenerator output voltage (see Fig. 6). This buffer can be realized by using a power operational amplifier in voltage follower mode. Further, it can be mentioned that the self-resistance and self-inductance of the electromagnetic

microgenerator are very small, therefore, the self-impedance of the microgenerators are not included for the analysis of the proposed converter operation. However, it can be incorporated in the analysis, for the prediction of the performances of the entire

energy harvesting system.

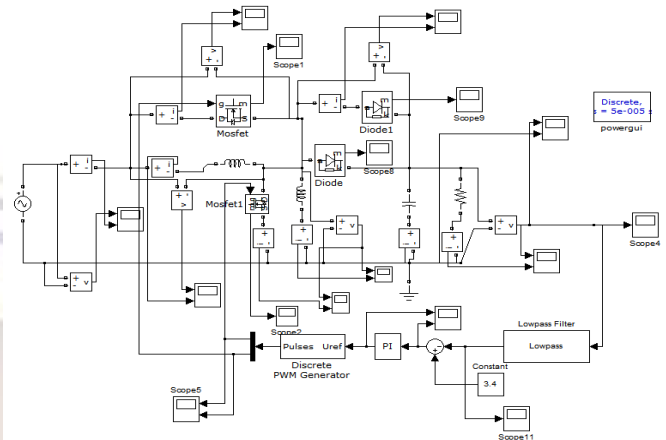


Fig 6. Circuit diagram of the energy harvesting converter

TABLE I
CIRCUIT COMPONENTS OF THE CONVERTER

Circuit Components	Name	Ratings
Inductor	L_1, L_2	4.7uH
Inductor resistance	R_L	30 mΩ
N - channel MOSFET	S_1, S_2	20V , 2A
MOSFET on state resistance	R_{ds_on}	150 mΩ @ $V_{gs}=3V$
Schottky Diode	$D_1 & D_2$	23V, 1A
Schottky Diode forward voltage	V_f	0.23V
Load resistance	R	200Ω
Capacitor	C	68 uF
Capacitor ESR	R_c	30 mΩ

The converter design is carried out based on the analysis and design guidelines, discussed earlier in the Sections II. Commercially available MOSFET (Si3900DV from Vishay) is selected to realize the switches S_1 and S_2 . The forward voltage of the selected MOSFET body diode is about 0.8 V, which is higher than the peak of the input voltage. This inhibits any reverse conduction in the MOSFETs. The nominal duty cycle of the converter is chosen to be 0.7. The inductor is designed to have a standard value of $4.7 \mu H$ and commercially available inductor (IHLP-2525CZ from Vishay) is used to realize L_1 and L_2 . Based on these designed values, the

switching frequency of the converter is selected to be 50 kHz. The diodes, D_1 and D_2 are chosen to be schottky type with low forward voltage (0.23 V, NSR0320 from ON Semiconductor). The output capacitor value is $68 \mu\text{F}$. The converter simulations are carried out in *Saber*. Circuit models of the selected devices and components, available from the manufacturers, are used in the simulations. Various values for circuit components of the designed converter are presented in Table I. To verify the proposed control techniques, at first simulation is carried out for the control scheme1, using $L_2 = L_1 = 4.7 \mu\text{H}$ and the duty ratio of the two converters are not equal. In the simulation, the duty cycle of the boost converter D_b is estimated by a PI controller (see Fig. 4). The buck-boost converter duty cycle D_c is calculated from the estimated duty cycle D_b . The input current of the boost converter (see i_b in Fig. 4) and the input current of the buck-boost converter (see i_c in Fig. 4) for load resistance $R = 200 \Omega$ is shown in Fig. 7(a) and (b), respectively. The total input current and the microgenerator output voltage (v_i) are shown in Fig. 7(c). It can be seen that the boost converter is operated during the positive half cycle, while the buck-boost converter is operated during negative half cycle of the microgenerator output voltage. The converter output voltage is shown in Fig. 8. The simulation output voltage of the energy harvesting circuit is shown in fig 9.

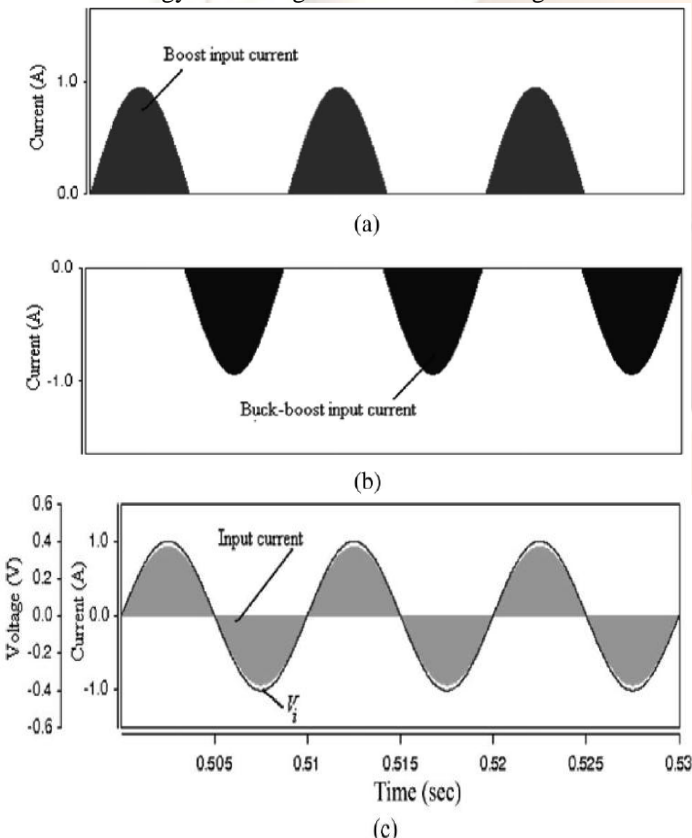


Fig. 7. (a) Boost input current, (b) buck-boost input current, and (c) total input current with ac input voltage for $R = 200 \Omega$ and $L_1 = L_2$.

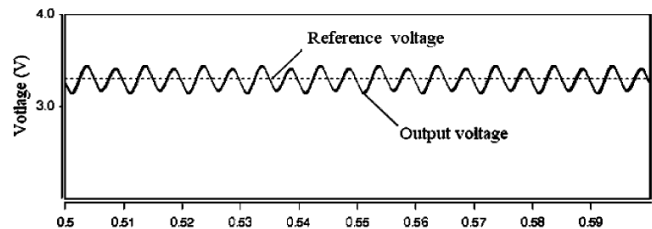


Fig.8. (a) Output voltage for $R = 200 \Omega$ and $L_1 = L_2$.

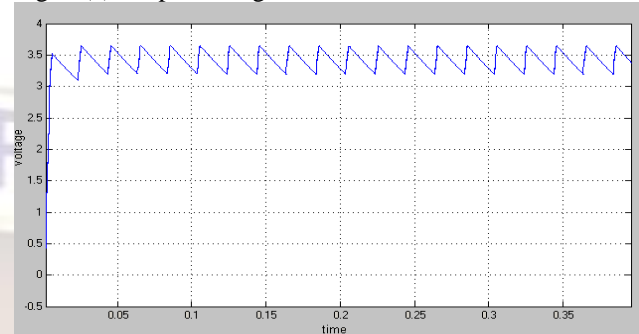


Fig 9. Simulation output voltage of energy harvesting circuit at $R=200\Omega$

The converter is also tested for a higher load resistance $R=400\Omega$. By testing the higher load resistance the ripple content at $R=200\Omega$ is neglected in $R=400\Omega$, that is upto 1.091. The output voltage of the $R=400\Omega$ can be shown as in fig.10.

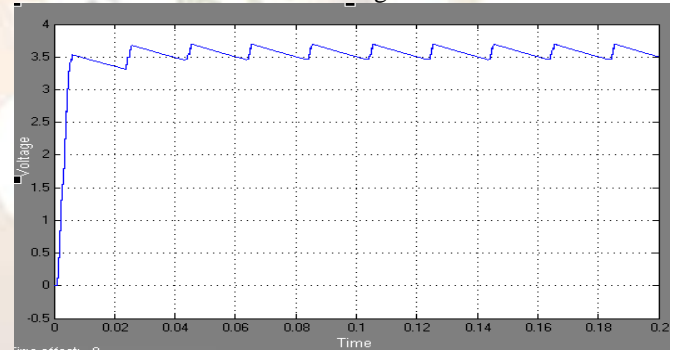


Fig 10. Simulation output of the energy harvesting circuit at $R=400\Omega$

IV. EXPERIMENTAL RESULTS

The circuit is further tested for input voltage 50V, the output can be expected as near to 200V. The simulation result of the energy harvesting circuit at the voltage of 50V can be shown in Fig.11.

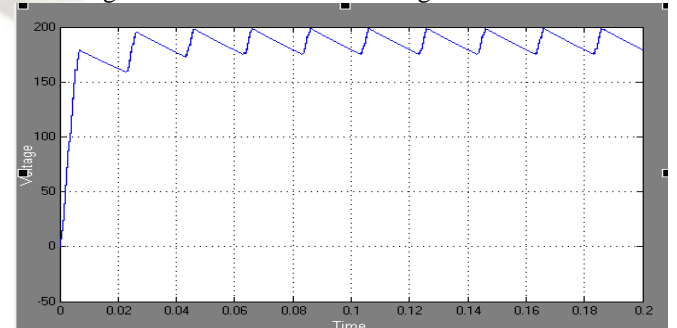


Fig.11. simulation output voltage of the energy harvesting circuit at input voltage 50V.

To calculate the power losses in the various components of the converter, the currents in the components of the converter circuits were measured and the values of the parasitic components (see Table I) were estimated. The measured currents, voltages, and the estimated component values were used to calculate the loss components analytically. In Table II, various loss components of the converter for the load resistance $R = 200 \Omega$ are presented. The power consumed by the entire control circuit is estimated. From this loss analysis, the estimated converter efficiency is 63.8%. This estimation agrees with the measurements and earlier simulation results. Further, it is found that in the case of inductor loss, about 70% of the total loss is due to the copper loss and the remaining 30% loss is due to the magnetic losses. Hence, with proper design of the conductor and the magnetic components, the converter efficiency can be improved. In the case of MOSFET loss, about 93% of the total loss is caused by the conduction loss and the remaining loss is due to the switching loss. Therefore, with the use of larger MOSFETs with lower ON-state resistance ($R_{ds\text{ ON}}$), the efficiency can be further improved. It can be noted that the efficiency of the converter, proposed in this study, is higher than the efficiency of the reported energy harvesting converters (44% in [20]).

TABLE II
LOSS CALCULATION

Components	Name	Estimated loss
Inductor (boost)	L_1	4.7 mW
Inductor (buck-boost)	L_2	4.9 mW
N - channel MOSFET (boost)	S_1	6.2 mW
N - channel MOSFET (buck-boost)	S_2	6.3 mW
Schottky Diode (boost)	D_1	2.4 mW
Schottky Diode (buck-boost)	D_2	2.5 mw
Output capacitor	C	0.1 mW
Control circuit	-	2.2 mW
PCB track resistance and contact resistances	-	1.6 mW
	<i>Total loss</i>	30.3 mW

V. CONCLUSION

The presented direct ac-to-dc low voltage energy-harvesting converter avoids the conventional bridge rectification and achieves higher efficiency. The proposed converter consists of a boost converter in parallel with a buck-boost converter. The negative gain of the buck-boost converter is utilized to boost the voltage of the negative half cycle of the

microgenerator to positive dc voltage. Operation of on state resistance efficiency has been improved. the proposed converter can also be successfully used for maximum energy harvesting.

REFERENCES

- [1] J. A. Paradiso and T. Starner, "Energy scavenging for mobile and wireless electronics," *IEEE Pervasive Comput.*, vol. 4, no. 1, pp. 18–27, Jan./Mar. 2005.
- [2] S. Meninger, J. O. Mur-Miranda, R. Amirtharajah, A. P. Chandrakasan, and J. H. Lang, "Vibration-to-electric energy conversion," *IEEE Trans. Very Large Scale Integr. Syst.*, vol. 9, no. 1, pp. 64–76, Feb. 2001.
- [3] M. El-Hami, P. Glynne-Jones, N. M. White, M. Hill, S. Beeby, E. James, A. D. Brown, and J. N. Ross, "Design and fabrication of a new vibration based electromechanical power generator," *Sens. Actuators A: Phys.*, vol. 92, pp. 335–342, 2001.
- [4] T. M. Thul, S. Dwari, R. D. Lorenz, and L. Parsa, "Energy harvesting and efficient power generation from human activities," in *Proc. Center Power Electron. Syst. (CPES) Semin.*, Apr. 2007, pp. 452–456.
- [5] N. G. Stephen, "On energy harvesting from ambient vibration," *J. Sound Vibrations*, vol. 293, pp. 409–425, 2006.
- [6] J. R. Amirtharajah and A. P. Chandrakasan, "Self-powered signal processing using vibration-based power generation," *IEEE J. Solid-State Circuits*, vol. 33, no. 5, pp. 687–695, May 1998.
- [7] B. H. Stark, P. D. Mitcheson, M. Peng, T. C. Green, E. Yeatman, and A. S. Holmes, "Converter circuit design, semiconductor device selection and analysis of parasitics for micropower electrostatic generators," *IEEE Trans. Power Electron.*, vol. 21, no. 1, pp. 27–37, Jan. 2006.
- [8] C. B. Williams and R. B. Yates, "Analysis of a micro-electric generator for microsystems," in *Proc. Int. Conf. Solid-State Sens. Actuators*, 1995, pp. 369–372.
- [9] P.D.Mitcheson, T. C. Green, E.M.Yeatman, and A. S. Holmes, "Architectures for vibration-driven micropower generators," *J. Microelectromech. Syst.*, vol. 13, no. 3, pp. 429–440, Jun. 2004.
- [10] S. Xu, K. D. T. Ngo, T. Nishida, G. B. Chung, and A. Sharma, "Low frequency pulsed resonant converter for energy harvesting," *IEEE Trans Power Electron.*, vol. 22, no. 1, pp. 63–68, Jan. 2007.
- [11] J. Elmes, V. Gaydarzhiev, A. Mensah, K. Rustom, J. Shen, and I. Batarseh, "Maximum energy harvesting control for

- oscillating energy harvesting systems," in *Proc. IEEE Power Electron. Spec. Conf.*, Jun. 2007, pp. 2792–2798.
- [12] S. P. Beeby, R. N. Torah, M. J. Tudor, P. Glynne-Jones, T. O'Donnell, C. R. Saha, and S. Roy, "Micro electromagnetic generator for vibration energy harvesting," *J. Micromech. Microeng.*, vol. 17, pp. 1257–1265, 2007.
- [13] B. H. Stark, P. D. Mitcheson, M. Peng, T. C. Green, E. Yeatman, and A. S. Holmes, "Converter circuit design, semiconductor device selection and analysis of parasitics for micropower electrostatic generators," *IEEE Trans. Power Electron.*, vol. 21, no. 1, pp. 27–37, Jan. 2006.
- [14] T. Paing, J. Shin, R. Zane, and Z. Popovic, "Resistor emulation approach to low-power RF energy harvesting," *IEEE Trans. Power Electron.*, vol. 23, no. 3, pp. 1494–1501, May 2008.
- [15] E. Lefevre, D. Audigier, C. Richard, and D. Guyomar, "Buck-boost converter for sensorless power optimization of piezoelectric energy harvester," *IEEE Trans. Power Electron.*, vol. 22, no. 5, pp. 2018–2025, Sep. 2007.
- [16] X. Cao, W.-J. Chiang, Y.-C. King, and Y.-K. Lee, "Electromagnetic energy harvesting circuit with feedforward and feedback DC–DC PWM boost converter for vibration power generator system," *IEEE Trans. Power Electron.*, vol. 22, no. 2, pp. 679–685, Mar. 2007.
- [17] G. K. Ottman, H. F. Hofmann, and G. A. Lesieutre, "Optimized piezoelectric energy harvesting circuit using step-down converter in discontinuous conduction mode," *IEEE Trans. Power Electron.*, vol. 18, no. 2, pp. 696–703, Mar. 2003.
- [18] G. K. Ottman, H. F. Hofmann, A. C. Bhatt, and G. A. Lesieutre, "Adaptive piezoelectric energy harvesting circuit for wireless remote power supply," *IEEE Trans. Power Electron.*, vol. 17, no. 5, pp. 669–676, Sep. 2002.
- [19] M. Ferrari, V. Ferrari, D. Marioli, and A. Taroni, "Modeling, fabrication and performance measurements of a piezoelectric energy converter for power harvesting in autonomous microsystems," *IEEE Trans. Instrum. Meas.*, vol. 55, no. 6, pp. 2096–2101, Dec. 2006.
- [20] P. D. Mitcheson, T. C. Green, E. M. Yeatman, and A. S. Holmes, "Power processing circuits for electromagnetic, electrostatic and piezoelectric inertial energy scavengers," *Microsyst. Technol.*, vol. 13, pp. 1629–1635, May 2007.
- [21] S. Dwari, R. Dayal, and L. Parsa, "A novel direct AC/DC converter for efficient low voltage energy harvesting," in *Proc. IEEE Ind. Electron. Soc. Annu. Conf.*, Nov. 2008, pp. 484–488.
- [22] A. Richelli, L. Colalongo, S. Tonoli, and Z.M. Kovacs-Vajna, "A 0.2–1.2 VDC/DC boost converter for power harvesting applications," *IEEE Trans. Power Electron.*, vol. 24, no. 6, pp. 1541–1546, Jun. 2009.
- [23] J. C. Salmon, "Circuit topologies for single-phase voltage-doubler boost rectifiers," *IEEE Trans. Power Electron.*, vol. 8, no. 4, pp. 521–529, Oct 1993.



G.Laxminarayana received the B. Tech. degree in Electrical and Electronics Engineering from JNT University and M.Tech in Power Electronics Engineering in Aurora's Engineering College (JNTU Hyderabad). He is currently working as a Assistant Professor in Aurora's Engineering College. He is working toward the Ph.D. degree in Electrical Engineering.



G.Bharagvi received the B. Tech. degree in Electrical and Electronics Engineering from JNTU and pursuing M.Tech in Power Electronics in Aurora's Engineering College (JNTU Hyderabad).